

THE ORBITAL SIPHON: A NEW SPACE ELEVATOR CONCEPT*

Colin R McInnes

Department of Mechanical Engineering, University of Strathclyde, Glasgow, G1 1XJ, UK,
colin.mcinnnes@strath.ac.uk

Chris Davis

Software Consultant, Devon, UK, cfd@idlex.freemove.co.uk

ABSTRACT

A new concept for propellantless payload transfer from the surface of the Earth to Earth escape is presented. Firstly, a simple model of a payload ascending or descending a conventional space elevator is developed to explore the underlying dynamics of the problem. It is shown that an unconstrained payload at rest on a space elevator at synchronous radius is in an unstable equilibrium, and that this instability can be used to motivate the development of a new concept for payload transfer. It will be shown that a chain of connected payloads stretching from the surface of the Earth to beyond synchronous radius can be assembled which will lift new payloads at the bottom of the chain, while releasing payloads from the top of the chain. The complete system therefore acts as an ‘orbital siphon’, transporting mass from the surface of the Earth to Earth escape without the need for external work to be done. Indeed the system performs net work by transferring energy from the Earth’s rotation to the escaping mass. The dynamics of the siphon effect are explored and key engineering issues are identified.

KEY WORDS: orbital tower, payload transfer, orbital dynamics

1. INTRODUCTION

The concept of an orbital tower has been discussed in the literature by many authors over a number of years. While the concept is clearly futuristic, interest has recently been revived due to advances in materials science (see for example [1-4]). In this paper, a simple model of a payload

* *Aspects of this work were presented as paper IAC-05-D4.2.07 “Novel Payload Dynamics on Space Elevator Systems”, 56th International Astronautical Congress, Fukuoka, October 2005.*

freely ascending or descending a space elevator will be considered to explore the underlying dynamics of the problem. Firstly, it will be shown that an unconstrained payload at rest on a space elevator at synchronous radius is in an unstable equilibrium. This instability is due to the presence of a maximum in the effective potential of the problem, which represents the gravitational and centripetal forces acting on the payload. The existence of this maximum in the effective potential then leads to a barrier which must be crossed by payloads ascending or descending the elevator. Conditions can be found which allow, for example, a payload captured at the top of the elevator to freely descend through synchronous radius. Similar conditions can also be determined under which a payload ascending the elevator will coast through synchronous radius and ascend the elevator to escape [5].

A more complex problem will then be investigated with a chain of payloads attached together along their length. New conditions can then be found under which the uppermost payloads will pull the lower payloads across the potential barrier noted above, and along the elevator to escape. A continuous chain of such payloads can be envisaged with new masses being added to the bottom of the chain as masses are released from the top of the chain and escape. The assembly then provides a continuous stream of mass lifted from the surface of the Earth and delivered to Earth escape without the need for external work to be done. It can be shown that the system in fact performs net work by transferring energy from the Earth's rotation to the escaping mass stream. In this light the ascending chain can be seen as a machine which leverages (siphons) energy from the Earth's rotation to the escaping mass stream [6]. While there are significant engineering difficulties associated with this concept, the underlying dynamics demonstrates that such an 'orbital siphon' is in principle possible and offers the prospect of the continuous delivery of mass from the surface of the Earth without the input of external work.

The orbital siphon idea was first developed by Davis in 1991, as part of a concept for transferring material from the surface of a rapidly spinning asteroid. It was noted that it may be possible to draw up a continuous train of material from the asteroid surface to escape. In 1996, (with the assistance of Dr Andrew Gay), a numerical simulation was developed with a chain of masses attached to the Earth's equator. Using this model, the operation of a simple orbital siphon was demonstrated and published on the web in 1997 [7]. In 2005 McInnes conducted an analysis of the dynamics of the siphon and McInnes and Davis co-

authored a paper that outlined the siphon principle at IAC 2005 [6]. In 2006, Davis developed an improved siphon simulation model, and made several further suggestions concerning siphon engineering issues [8]. A related concept was set out by Logsdon [9] the same year that the orbital siphon simulation was first published on the web. However Logsdon's SkyHook Pipeline requires pumps to raise water to geosynchronous orbit, after which the water 'falls' outward to drive turbines that generate more than sufficient power to drive the pumps, and could thus provide net electrical power generation. The siphon, by contrast, is simply a long chain of tethered masses, and requires no pumps or external work for its operation once the siphon is in operation.

2. DYNAMICS OF A SINGLE MASS

In order to motivate the idea of the orbital siphon, a single point mass is considered moving along a tether of length L , assuming that the tether is rigid and co-rotates with the Earth (radius R_E) at constant angular velocity Ω , as shown in Fig. 1. As the mass moves along the tether, it experiences a transverse coriolis force resulting in friction between the particle and tether [5].

For the frictionless case, the effective potential ϕ is the sum of the gravitational potential of the Earth and a potential which represents the centripetal acceleration defined as

$$\phi(R) = -\frac{1}{2}R^2\Omega^2 - \frac{\mu}{R} \quad (1)$$

where μ is the gravitational parameter of the Earth and R is the distance of the particle from the centre of the Earth. This 1-dimensional problem is conservative and can be described by a 2-dimensional phase space with Hamiltonian $\mathcal{H}(R, \dot{R})$ defined by

$$\mathcal{H}(R, \dot{R}) = \frac{1}{2}\dot{R}^2 + \phi(R) \quad (2)$$

Because the system is conservative $\dot{\mathcal{H}}(R, \dot{R}) = 0$ and the problem immediately presents an integral of motion given by $\mathcal{H}(R, \dot{R}) = C$ so that

$$C = \frac{1}{2}\dot{R}^2 - \frac{1}{2}R^2\Omega^2 - \frac{\mu}{R} \quad (3)$$

This integral allows the phase space of the problem to be explored for level curves of C . Then, the equation of motion of the particle can be determined from the Hamiltonian using $\dot{R} = \partial\mathcal{H}/\partial\dot{R}$ and $\ddot{R} = -\partial\mathcal{H}/\partial R$ which yields

$$\ddot{R} = R\Omega^2 - \frac{\mu}{R^2} \quad (4)$$

It is clear from Eq. (4) that a single equilibrium point exists when the radial acceleration vanishes at the point $R = \bar{R}$, defined by

$$\frac{\partial\mathcal{H}(R, \dot{R})}{\partial R} = 0 \Rightarrow \bar{R} = \left[\frac{\mu}{\Omega^2} \right]^{1/3} \quad (5)$$

which corresponds to a single equilibrium point E at synchronous radius (6.6 Earth radii). The nature of this equilibrium point can now be determined from the Hamiltonian [10]. To demonstrate this, the class of turning point of the Hamiltonian can be found from

$$\begin{aligned} q(R) &= \frac{\partial^2\mathcal{H}}{\partial R^2} \frac{\partial^2\mathcal{H}}{\partial \dot{R}^2} - \left[\frac{\partial^2\mathcal{H}}{\partial R\partial\dot{R}} \right]^2 \\ &= -\Omega^2 - \frac{2\mu}{R^3} \end{aligned} \quad (6)$$

so that, substituting Eq. (5), $q(\bar{R}) = -3\Omega^2$ demonstrating that the equilibrium point is hyperbolic (\mathcal{H} has a saddle point at $R = \bar{R}$) and unstable. The eigenvalues λ of the linear system in the neighbourhood of the hyperbolic point E can also be determined from the characteristic polynomial P defined by [10]

$$P(\lambda) = \left\| \begin{bmatrix} \frac{\partial^2 \mathcal{H}}{\partial R \partial \dot{R}} & \frac{\partial^2 \mathcal{H}}{\partial \dot{R}^2} \\ -\frac{\partial^2 \mathcal{H}}{\partial R^2} & -\frac{\partial^2 \mathcal{H}}{\partial R \partial \dot{R}} \end{bmatrix} - \lambda I_{2 \times 2} \right\| = 0 \quad (7)$$

which, from Eq. (2), reduces to

$$\lambda = \pm \sqrt{-\frac{\partial^2 \mathcal{H}}{\partial R^2}} \Big|_{R=\bar{R}} = \pm \sqrt{3} \Omega \quad (8)$$

This pair of real eigenvalues correspond to stable ($-\sqrt{3}\Omega$) and unstable ($+\sqrt{3}\Omega$) manifolds attached to E , shown in Fig 2. Because E is a saddle point, it represents a potential barrier to particles attempting to transit it from either direction along the tether, represented by the transit and no-transit phase paths shown in Fig. 2. Level curves parameterised by C are shown in Fig. 3, where the equilibrium E corresponds to a hyperbolic fixed point. The stable and unstable manifolds are a linearization of the separatrix K which discriminates globally between transit and no-transit paths.

Because the Hamiltonian of the problem forms an integral, the radial speed V of a particle moving freely along the tether can be obtained from Eq. (3) as

$$V(R)^2 = R^2 \Omega^2 + \frac{2\mu}{R} + 2C \quad (9)$$

while the transverse speed U is given by

$$U(R)^2 = R^2 \Omega^2 \quad (10)$$

Therefore, the angle γ of the absolute velocity of the particle relative to the tether can be written as

$$\tan \gamma(R) = \frac{R\Omega}{\sqrt{R^2\Omega^2 + \frac{2\mu}{R} + 2C}} \rightarrow 1 \quad (11)$$

which yields the limit $\gamma \rightarrow \pi/4$ for large R . Similarly, the absolute speed of the particle W can be obtained from Eq. (9) and Eq. (10) as

$$W(R) = \sqrt{2R^2\Omega^2 + \frac{2\mu}{R} + 2C} \rightarrow \sqrt{2}R\Omega \quad (12)$$

which yields a limiting speed of $\sqrt{2}R\Omega$ for large R .

For particles moving down the tether, after being captured at the end, the effective particle energy C must be such that the particle can cross the potential barrier at E and avoid being reflected back on a no-transit phase trajectory. Evaluating C at E, the following function can be defined

$$f(\xi) = \sqrt{\Omega^2(\xi^2 - \bar{R}^2) + 2\mu\left(\frac{1}{\xi} - \frac{1}{\bar{R}}\right)} \quad (13)$$

for arbitrary ξ , such that to ensure transit of E it is required that $-V(L) > f(L)$. Similarly, for particles ascending the tether under power, if $V(R) > f(R)$ then the particle will pass through E and escape with no further external work required. Clearly, there are issues concerning the optimum strategy to ascend and descend the tower (minimum-time, minimum-energy), however these are beyond the scope of this paper.

3. DYNAMICS OF A CHAIN OF MASSES

The analysis for a single mass can now be extended to a chain of N masses, as shown in Fig. 4. Each element of the chain comprises a mass m connected to neighbouring masses by a (assumed massless) tether of length d . An individual mass in the chain will experience gravitational and centripetal forces, in addition to internal tension forces from its nearest neighbours in the chain.

For an appropriate number of mass elements and mass spacing the entire system can be configured to remain in equilibrium. The resultant gravitational and centripetal forces acting along the system then balance. This is a discrete form of the continuous hanging tower defined by Pearson [1].

Consider now the effect of increasing the length of the tower beyond that required for equilibrium. Then, there will be an excess of centripetal force acting on the chain of masses above synchronous orbit which can be used to lift new payloads from the surface of the Earth, as shown in Fig 5. The masses which are beyond synchronous orbit are driving the lower masses in the chain across the effective potential barrier, discussed earlier for the single mass case. An ‘orbital siphon effect’ can then be established where as a new payload is added to the bottom of the chain, a payload is released from the top so that the overall length of the chain does not change. However, there is a net radial force which will maintain the flow of mass from the surface of the Earth to Earth escape.

The total force acting on each mass in the chain can be determined from the sum of the gravitational and centripetal forces along with the tension forces exerted by the nearest neighbours on the chain. For the j^{th} mass, the total force is given by

$$f_j = \frac{-GMm}{(R_E + jd)^2} + m\Omega^2(R_E + jd) \quad (14)$$

The internal tension forces are not explicitly listed here since they will vanish during a summation over the chain of masses to be performed later. In non-dimensional form the force on the j^{th} mass can then be written as

$$\bar{f}_j = \frac{-1}{(1 + \lambda j)^2} + \Lambda(1 + \lambda j) \quad (15a)$$

$$\bar{f}_j = \frac{R_E^2}{GMm} f_j, \lambda = \frac{d}{R_E}, \Lambda = \frac{\Omega^2 R_E^3}{GM} \quad (15b)$$

where Λ is the ratio of the centripetal and gravitational forces exerted on a mass at R_E . In order

to determine the conditions for equilibrium in the chain of masses, the net resultant force can be found from the summation

$$F = \sum_{j=0}^N \bar{f}_j \quad (16)$$

Then, performing the summation using Eq. (15), it can be shown that the net resultant force on the chain of masses is given by

$$F = \frac{1}{2} \Lambda(1+N)(2 + \lambda N) + \frac{1}{\lambda^2} [\psi^{(1)}(1+1/\lambda + N) - \psi^{(1)}(1/\lambda)] \quad (17)$$

where $\psi^{(m)}(z)$ is the polygamma function, defined in series form as

$$\psi^{(m)}(z) = (-1)^{m+1} m! \sum_{k=0}^{\infty} (z+k)^{-(m+1)} \quad (18)$$

The condition for equilibrium of the chain of masses can then be found from

$$F = \sum_{j=0}^N \bar{f}_j = 0 \quad (19)$$

This requirement then defines the length of the chain for a given number of masses N , as listed in Table 1. It can be seen that for a large number of masses the length of the chain approaches that defined by Pearson for a continuous hanging tower [1]. The net non-dimensional force acting on a chain with $N=1000$ is shown in Fig. 6. It can be seen that the chain will be in equilibrium for a given length (22.7 Earth radii). If the chain is longer than this equilibrium length the chain will rise, while if the chain is shorter the chain will fall, resulting in an unstable equilibrium as

expected from the analysis of a single mass (see also [11]).

The orbital siphon effect described here utilises the excess centripetal force acting on the chain of masses above synchronous orbit to lift new payloads from the surface of the Earth. The parameter Λ is therefore an important measure of the performance of such a system. It can be seen from Table 2. that the Earth is clearly the most attractive terrestrial planet for such a system, although the same principles could be used effectively on asteroids to deliver mass to escape in a continuous stream.

4. ORBITAL SIPHON OPERATION

4.1 Numerical Simulation Model Considerations

The first 2D orbital siphon simulation model [7] began as a static radial chain of masses tied together by massless cables, the motion of which over small intervals of time was calculated using inverse square gravity, and Hooke's law. The model was initialised as a stationary radial tower with some 25 masses connected by equal length massless elastic ties along a 250,000 km radius chain. The chain was then released at the base and allowed to freely accelerate and pull up further masses from the equator of the Earth. However, it was found that the rising chain of masses deflected from radial, and stopped pulling up new payload masses from the base, and either reeled back down or entirely collapsed.

A solution to this issue is to constrain the rising chain to a radial path by simply restricting tangential velocities to the angular velocity of the Earth (but without stating how this is achieved at present), effectively holding the mass chain rigidly to a radial path. With this modification in place, simulation shows that a rising chain will pull up masses from the base, while releasing them from the top. However, the rising chain continues accelerating, pulling up masses from the base faster and faster. A solution to this second issue is to constrain the lowest mass in the rising chain to some peak radial speed, using a braking system. With these two modifications in place, the principal problem becomes that of strong radial oscillations within the rising chain. In part this arises from the application of the brake on the lowest body, the lifting of new masses onto the chain at the base, and to a smaller extent the release of masses from the top of the chain. Radial oscillations in the chain can be controlled by ensuring that the chain accelerates slowly up to operating speed so that only modest braking is required in normal

operation, and to accelerate new masses up to the operating radial velocity before attaching them to the rising chain. The result of these modifications is a smoothly operating siphon simulation model [8].

The simulation (Fig. 7) displays the rising siphon chain of masses, and the tension, radial velocity, radial acceleration, and transverse coriolis force. The tension maximum is shown to remain at synchronous radius, and the radial speed remains uniform along the length of the chain. The coriolis force, which acts against the rotation of the chain, is calculated by recovering the accelerations discarded to maintain the radial motion of the siphon.

4.2 Engineering Considerations

The engineering issues which arise with the orbital siphon concept can be addressed, at least in outline. The first issue is how to lend the siphon sufficient rigidity to overcome the coriolis forces deflecting it as it rises. Since coriolis force is constant along the length of the siphon, at $F_C = 2m\Omega v$, for mass element m and radial speed v , coriolis forces can clearly be minimized by using masses rising at low radial velocities. It is probably not necessary for the rising chain to be maintained exactly radial, and it can be allowed to bend back from the direction of rotation to some extent. Indeed, some numerical studies suggest that a non-rigid siphon will indeed raise small masses rising at low speeds, with the rising mass chain deflecting back from radial. However, if larger masses and higher speeds are required, some degree of stiffness is likely required along the mass chain. Several solutions are proposed:

- A cantilever truss along the length of the siphon mass chain, all of whose members would be in tension (Fig. 8).
- The mass chain itself to be a rising cantilever truss, with all its members in tension.
- Thrusters, mounted transversely on the mass chain used to counter the coriolis force.

The engineering problem of braking the siphon appears best resolved by feeding out the siphon from around the drum of an electric dynamo located at the base of the siphon. The base is the only location where any sort of conventional braking can be applied. The power output P from the dynamo would be of order $P \sim F_R v$ for a radial force F_R exerted by the siphon at its base, and radial speed of the siphon v .

The problem of damping radial oscillations appears best resolved by, firstly, using the dynamo brake to slow the rising siphon. Furthermore, the power generated by this brake may be sufficient to accelerate payload masses up to operating radial speed prior to attachment to the siphon. Finally, in order to minimize the oscillations due to payload release, payload masses should either be either minimized or incrementally released. This suggests that a siphon chain should consist of a chain of many small masses rather than few large masses.

These proposals offer outline engineering solutions to the problems uncovered during simulation studies. However, there are other issues which the simulation does not address, several of which are concerned with the tether. In the first place, the siphon as described so far would launch long lengths of tether needlessly to Earth escape along with the payload masses. One simple solution to this would be to use a tether loop, with one end wrapped round the brake dynamo drum at the base, and the top wrapped around a counterweight wheel or drum at the top (Fig. 9). In this manner, only payload masses would be released from the top of the siphon, and tether would cycle back. Such a solution offers the possibility of periodically replacing the tether loop should it become worn or damaged.

However, a further issue with both a single tether and a tether loop siphon is that such tethers must have a uniform cross-section along their length, while the tension maximum in the siphon is at synchronous radius. Fixed space elevator tethers are accordingly tapered for a maximum cross-sectional area at synchronous radius, to produce a constant stress along the tether. If this is also required for a siphon, then one possible way of 'tapering' a tether loop would be to introduce further tether loops inside the main tether loop, such that they meshed together to increase the cross-sectional area of the tether loop system at synchronous radius (Fig. 10). A further possibility would be to mount several tether loops adjacent to each other around the payload mass chain, tied together at their top, so as to distribute stress between them.

Given these various proposals for resolving the engineering problems associated with a siphon, they need to be combined together into an integrated system. One simple proposal is to mount a tether loop on a cantilever truss. The drum at the base would drive the dynamo brake, and an acceleration chamber below would be used to accelerate payloads before attaching to the rising siphon in order to reduce radial oscillations. The system would be oriented E-W to allow the truss to counter the coriolis force (Fig. 11).

The construction of such a siphon would begin with a tether loop space elevator, with the

dynamo acting as a motor to raise payloads. The entire system would then be extended by increasing the amount of tether ribbon in the tether loops, and constructing the cantilever truss once the required siphon altitude had been reached. The electric motors at the base would then begin raising payloads up the tether loop until the mass chain began to operate as a siphon, at which point the electric motors would become dynamo brakes.

The initial siphon payload cargo could also be made up of small masses that pulled up heavier ones, until operating payload masses were entrained in the siphon. Equally, in slowing and halting a siphon, the payload masses could be reduced, and the final siphon cargo might consist of small dummy payload masses, used simply to keep the siphon primed for subsequent use. An entire siphon payload train might consist of a head of small dummy masses, followed by an enlarging payload train, followed by a dwindling payload train, and a tail of small dummy masses. Payloads released into space from the siphon would likely not be sprayed in all directions, but retained in a lengthening payload train trailing from top of the siphon, to be daily released all together in some direction.

The principal advantage of an orbital siphon over a space elevator is that whereas a space elevator requires work to be done to raise masses to escape, an orbital siphon leverages energy from the Earth's rotation to raise a continuous stream of payload masses - and indeed acts to slow the rotation of the Earth.. The only work that is required is to give payloads an initial small radial velocity, and the siphon dynamo brakes may well produce sufficient power to do this as well. If payload launch costs for a space elevator are likely to be a small fraction of conventional rocket launches, the launch costs for a siphon are, in principle, zero. However, any siphon would have higher capital costs of construction than a space elevator, and their engineering and operation would be considerably more complex.

But, assuming that the engineering problems can be solved, an orbital siphon offers an ultra-cheap mass transport system into space. While space elevators could launch tens or hundreds of tons of payloads into space per annum, heavy duty siphons could in principle launch thousands of tons of payloads into space per annum in a continuous stream. If anything, the principal problem would become one of feeding sufficient numbers of payloads into the siphon to keep them running continuously.

5. CONCLUSIONS

A simple model has been used to investigate the dynamics of a single mass freely ascending or descending a space elevator system. By defining an effective potential for the problem, it has been shown that there exists a local maximum in this potential at synchronous radius. The analysis has then been extended to a chain of masses, where the uppermost masses are able to pull the lower masses across the potential barrier, resulting in an ‘orbital siphon’ effect. Numerical simulation shows that such a system poses practical challenges. However, in principle mass can be transported from the surface of the Earth to escape without the need for external mechanical work. This intriguing underlying principle offers scope for further investigation and development of the orbital siphon concept.

REFERENCES

- ¹J. Pearson, “The Orbital Tower: A Spacecraft Launcher Using the Earth’s Rotational Energy,” *Acta Astronautica*, Vol. 2, No. 9-10, 1975, pp. 785-799.
- ²A.C. Clarke, “The Space Elevator: Thought Experiment or Key to the Universe,” *Advanced Earth Oriented Applications of Space Technology*, Vol. 1, 1981, pp. 39-48.
- ³B.B. Edwards, “Design and Deployment of a Space Elevator,” *Acta Astronautica*, Vol. 47, No. 10, 2000, pp. 735-744.
- ⁴D.V. Smitherman, *Space Elevators: An Advanced Earth-Space Infrastructure for the New Millennium*, NASA Report CP-2000-210429, Marshall Space Flight Center, Huntsville, 2000.
- ⁵C.R. McInnes, “Dynamics of a Particle Moving Along an Orbital Tower,” *Journal of Guidance, Control and Dynamics*, Vol. 28, No. 2, 2005, pp. 380-382.
- ⁶C.R. McInnes, and C. Davis, “Novel Payload Dynamics on Space Elevator Systems,” IAC-05-D4.2.07, 56th International Astronautical Congress, Fukuoka, October 2005.
- ⁷<http://www.idlex.freemove.co.uk/siphon/siphon.html> (accessed 20 April 2006)
- ⁸http://www.idlex.freemove.co.uk/siphon/analytics/elevator/smooth_siphon.html (accessed 20 April 2006)
- ⁹T.S. Logsdon, *Orbital Mechanics: Theory and Applications*, Wiley, 1997, pp. 246-248.
- ¹⁰D.W. Jordan, and P. Smith, *Nonlinear Ordinary Differential Equations*, 3rd edition, Oxford University Press, Oxford, 1999, pp. 78-80.
- ¹¹A. Steindl, and H. Troger, Is the Sky-hook Configuration Stable, *Nonlinear Dynamics*, Vol. 40, No. 4, 2005, pp. 419-431.

Figure and Table Captions

Table 1: Mass chain length L required for equilibrium as a function of number of masses N .

Table 2: Parameter Λ (ratio of centripetal to gravitational force) for a range of bodies.

Fig. 1: Schematic space elevator of length L co-rotating with angular velocity Ω .

Fig. 2: Schematic hyperbolic fixed point E with stable (-) and unstable manifolds (+), transit (T) and no-transit (NT) phase paths.

Fig. 3: Phase paths for particles freely moving along a space elevator with separatrix K.

Fig. 4: Chain of N masses of length L co-rotating with angular velocity Ω .

Fig. 5: Schematic space elevator ‘orbital siphon’ effect.

Fig. 6: Resultant non-dimensional force acting on a chain of masses as a function of length ($N=2000$).

Fig. 7: Orbital siphon simulation for 250,000 km tower showing tension, radial velocity and acceleration, and Coriolis force.

Fig. 8: Cantilever truss siphon.

Fig. 9: Tether loop.

Fig. 10: Multiple tether loop.

Fig. 11 Combined multiple tether loop and cantilever truss siphon.

Table 1.

N	5	50	500	5000	∞
L (R_E)	95.51	25.91	22.92	22.68	22.65

Table 2.

Body	Mercury	Venus	Earth	Vesta
Λ	3.5×10^{-5}	5.8×10^{-4}	3.5×10^{-3}	0.78

Figure 1.

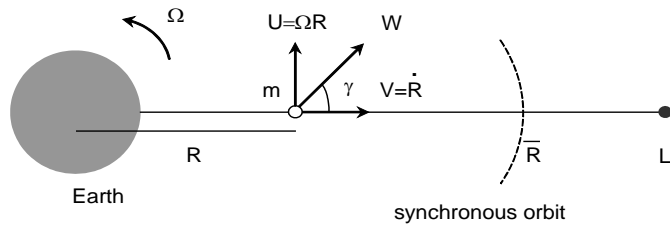


Figure 2.

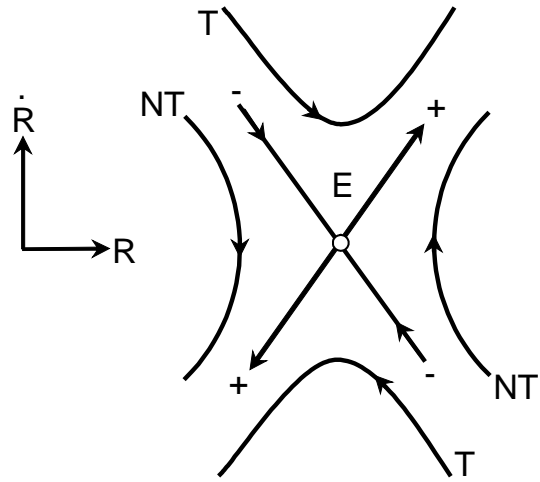


Figure 3.

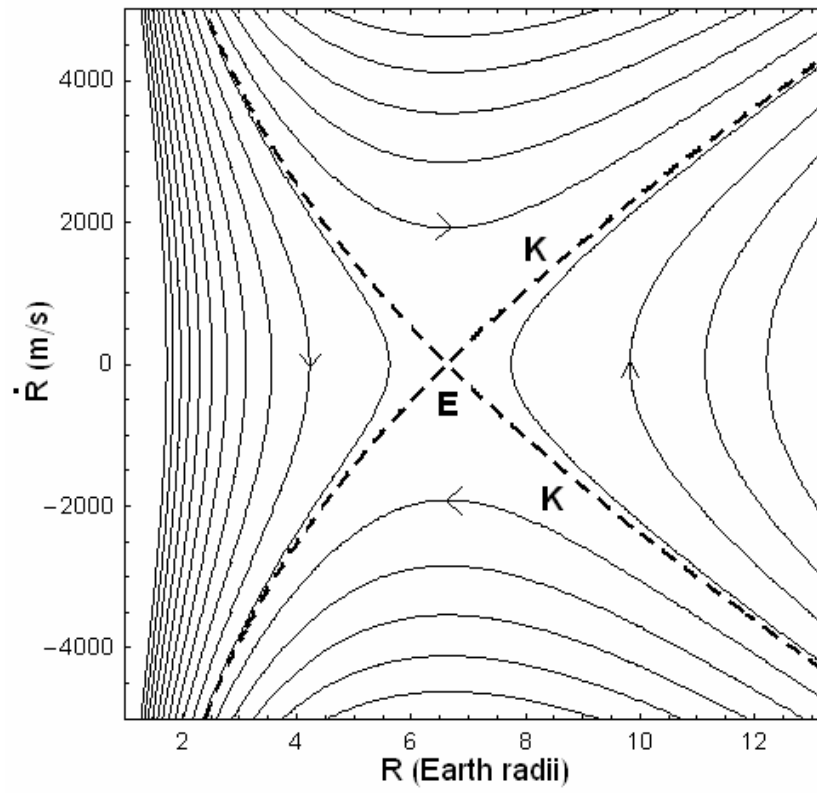


Figure 4.

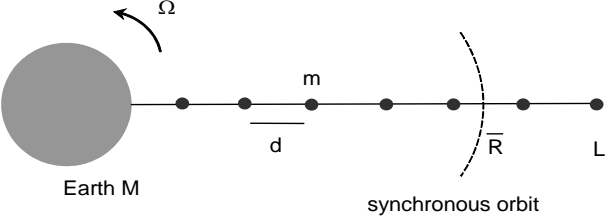


Figure 5.

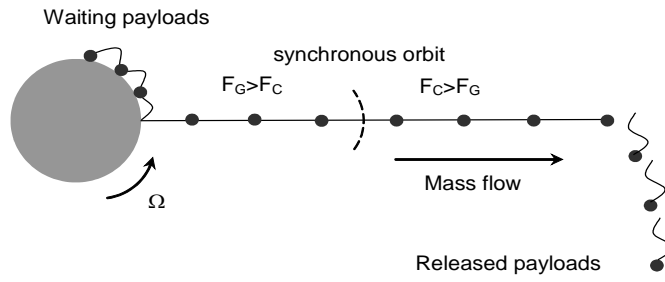


Figure 6.

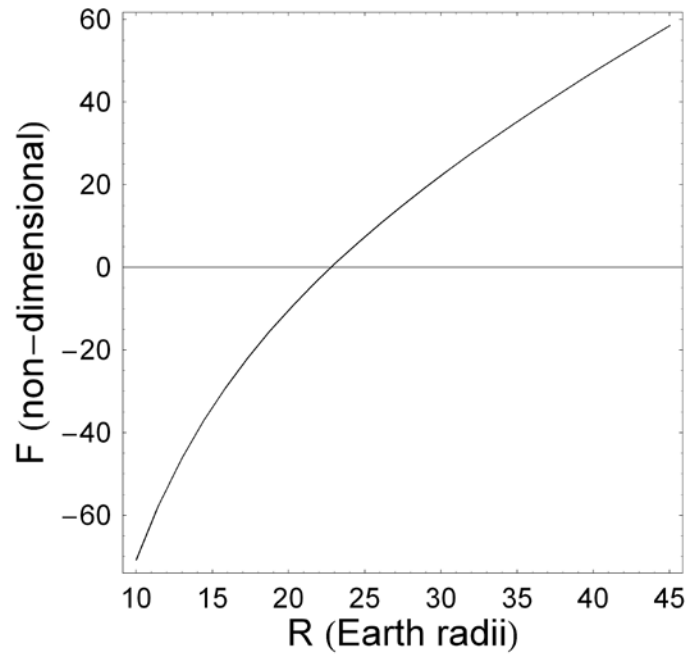


Figure 7.

250000 km Siphon Bead mass 1000 kg Tie len 10000 km XsectA 5.0E-4 m² YM 1000 GPa
Counterweight 250 kg Max radial velocity 2000.0 m/s Lowest tie tension 11463 N
777107 s DT 0.1 Brake power 22MW

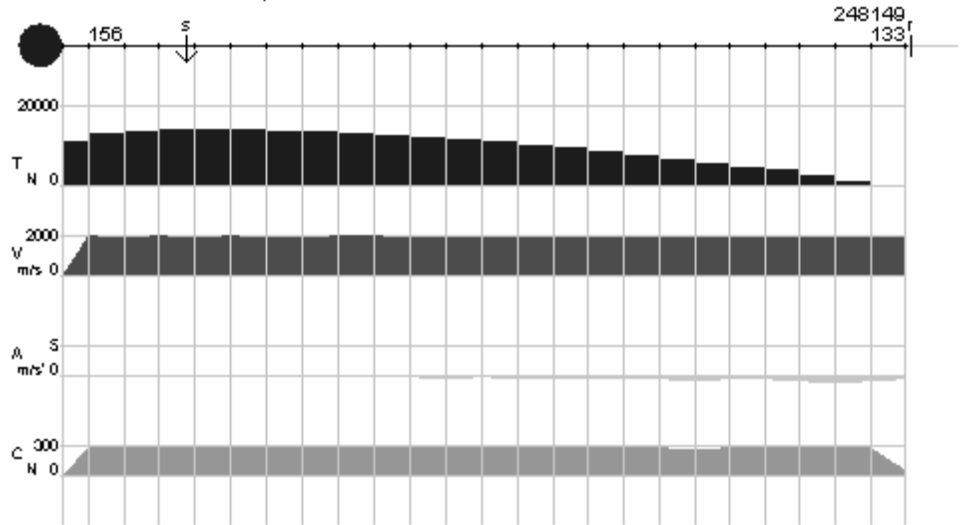


Figure 8.

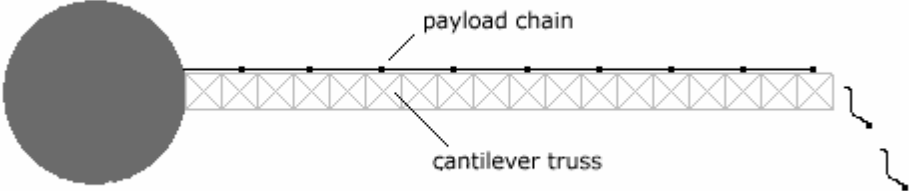


Figure 9.

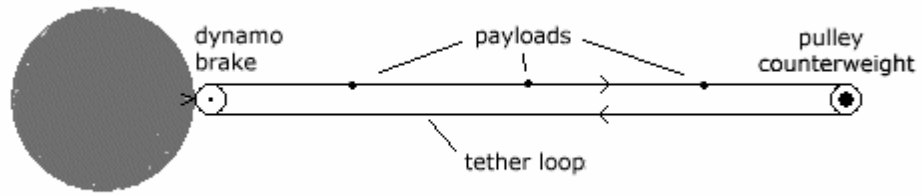


Figure 10.

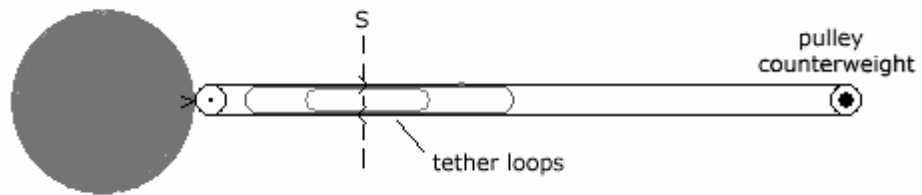


Figure 11.

